CHEMISTRY
A EUROPEAN JOURNAL

Synthesis of Ag and AgI Quantum Dots in AOT-Stabilized Water-in-CO_2 Microemulsions

Juncheng Liu,[a, b] Poovathinthodiyil Raveendran,[a, b] Zameer Shervani,[a, b] Yutaka Ikushima,*[a, b] and Yukiya Hakuta[a]

Abstract: Silver and silver iodide nanocrystals have been synthesized in the water-in-CO_2 reverse microemulsions formed by the commonly used surfactant, sodium bis(2-ethylhexyl)sulfosuccinate (AOT), in the presence of 2,2,3,3,4,4,5,5-octafluoro-1-pentanol as cosurfactant. The nanometer-sized aqueous domains in the microemulsion cores not only act as nanoreactors, but the surfactant interfacial monolayer also helps the stabilization of the metal and semiconductor nanoparticles. The transmission electron microscopy results show that silver and silver iodide nanocrystals with average diameters of 6.0 nm (standard deviation, SD = 1.3 nm) and 5.7 nm (SD = 1.4 nm), respectively, were formed. The results indicate that the method can be utilized as a general and economically viable approach for the synthesis of metal and semiconductor quantum dots in environmentally benign supercritical carbon dioxide.

Keywords: AOT · carbon dioxide · microemulsions · nanoparticles · supercritical fluids · surfactants

Introduction

Metal and semiconductor particles in the nanometer size range exhibit quantum confinement effects that give rise to unique electronic and optical properties useful for a variety of new technologies, including electronic, optical, biomedical, coating, catalytic, memory, and sensor applications.[1] However, the high surface energy of these particles makes them extremely reactive, and most systems undergo aggregation if their surfaces are without protection or passivation. To effectively utilize their size-dependent properties, the particle size and polydispersity must be controlled, and often organic capping agents, with proper binding strengths for the substrate, are used to passivate the particles' surfaces and quench particle growth. Some of the commonly used methods for surface passivation include protection by a self-assembled monolayer of thiol-functionalized organic molecules,[2] encapsulation in the polar core of reverse microemulsions (RMs),[3] and dispersion in polymeric matrices.[4]

RM cores are preferred templates for the synthesis of metal and semiconductor nanoparticles as they are thermodynamically stable, optically transparent solutions consisting of spatially defined aqueous nanodroplets, in which the nanoparticles can be compartmentally grown from their water-soluble precursors. Water-in-oil (w/o) RMs have been extensively used to synthesize metal and semiconductor nanoparticles.[3] However, a serious problem in using w/o RMs for nanoparticle synthesis is the separation and removal of solvent from the products. In the past decade, supercritical fluids (SCFs) have attracted considerable interest as a reaction medium to synthesize nanoparticles,[2d–f,5] because the variations in SCF solvent properties, such as density, diffusivity, viscosity, and dielectric constant, can be easily realized by changing the system temperature and pressure.[6] These adjustable properties thereby allow for the manipulation of the desired nanoparticle or nanowire morphology,[7] in consideration of the solvent effect on nanoparticle growth. Additionally, separation of the nanoparticles from the solvent is easily facilitated by decreasing the system pressure, thereby leading to direct deposition of nanoparticles without any solvent residue. Supercritical carbon dioxide ($scCO_2$) is the preferred reaction medium among SCFs from both economic and green chemistry perspectives, because it is naturally abundant, nontoxic, nonflammable, in-

[a] Dr. J. Liu, Dr. P. Raveendran, Dr. Z. Shervani, Prof. Dr. Y. Ikushima, Dr. Y. Hakuta
Supercritical Fluid Research Center
National Institute of Advanced Industrial Science and Technology
4–2–1 Nigatake, Miyagino-ku, Sendai 983–8551 (Japan)
Fax: (+81) 22-232-7002
E-mail: y-ikushima@aist.go.jp

[b] Dr. J. Liu, Dr. P. Raveendran, Dr. Z. Shervani, Prof. Dr. Y. Ikushima
CREST, Japan Science and Technology Agency
4–1–8 Honcho, Kawaguchi 332–0012 (Japan)

DOI: 10.1002/chem.200400508

expensive, and has a moderate critical temperature and pressure (31.1 °C and 7.38 MPa, respectively). Although CO_2 has a zero dipole moment and a low dielectric constant, it is a charge-separated molecular system,[8] which will result in low polarizability and considerable electrostatic interactions, and thus most of the hydrocarbon-based surfactants are not suitable for the CO_2/water interface.[9] Although examples of RMs guided by the steric-controlled design of hydrocarbon surfactants in $scCO_2$ have been reported,[10] in general, fluorocarbon tails are used for the enhanced stabilization of the surfactant tails in CO_2.[11] So far, several fluorinated surfactants, such as ammonium carboxylate perfluoropolyether $CF_3O(CF_2CF(CF_3)O)_3CF_2COO^-NH_4^+$ (PFPE NH_4^+),[12] the sodium salt of bis(2,2,3,3,4,4,5,5-octafluoro-1-pentyl)-2-sulfosuccinate(di-HCF_4),[13] and a mixture of sodium bis(2-ethylhexyl)sulfosuccinate (AOT) and perfluoropolyether-phosphate ether (PFPE-PO_4),[14] have been used to synthesize nanoparticles in $scCO_2$ through the formation of water-in-CO_2 (w/c) RMs. However, the high cost of these fluorocarbon surfactants make them less promising as industrially viable surfactant systems. Furthermore, the synthesis of monodisperse metal and semiconductor quantum dots has been a large challenge for these systems. Therefore, it is interesting to explore how to make commercially available surfactants form w/c RMs that can compartmentally grow monodisperse quantum dots in an $scCO_2$ bulk phase.

In the present work, we demonstrate the synthesis of relatively monodisperse metal and semiconductor nanocrystals within the quantum size domain (less than 10 nm), by using w/c RMs stabilized by AOT and a small amount of 2,2,3,3,4,4,5,5-octafluoro-1-pentanol (F-pentanol) as cosurfactant. The work reveals that cosolvent/cosurfactant effects can greatly aid in enabling the formation of RMs in $scCO_2$ at moderate pressures and low cost, and that these aqueous templates can be effectively used for the synthesis of metal and semiconductor quantum dots.

Results and Discussion

Silver nanocrystals: The silver nanoparticles were synthesized by the reduction of Ag^+ ions in the water core of the AOT/F-pentanol (AOTF) w/c RMs by using $NaBH(OAc)_3$. The acidic nature of the water core caused by the formation of carbonic acid made conventional reagents, such as $NaBH_4$ and hydrazine, unsuitable as they would react with CO_2 under the experimental conditions. The AOTF w/c RMs were prepared by mixing the AOT (0.016 M)/F-pentanol (0.24 M)/water/$scCO_2$ system at 38.0 °C and 34.50 MPa.[15] The water loading value, W ($W=[H_2O]/[surfactant]$), used in the experiments (corrected for the water dissolved in the $scCO_2$ continuous phase) for synthesizing silver and silver iodide nanocrystals was 4.7 and 5.6, respectively. Although the W value in the microemulsion system is not high under the experimental conditions, these nanometer-sized aqueous domains are particularly attractive for the synthesis of metal and semiconductor quantum dots below 10 nm in size; in this range the particles exhibit significant quantum-size effects on optical and electrical properties.

The AOTF w/c RM system ($W=4.7$) at 27.00 MPa and 38.0 °C was confirmed to be optically transparent and homogeneous. The appearance of a brown–yellow cloud was observed immediately after injecting the ethanolic solution of $NaBH(OAc)_3$. We suggest that this may be due to the chemical reaction leading to the formation of silver nanoparticles. After several minutes the cloud disappeared and the whole system became an optically transparent single phase again. The digital images showing the silver nanoparticle formation inside the view cell are presented in Figure 1.

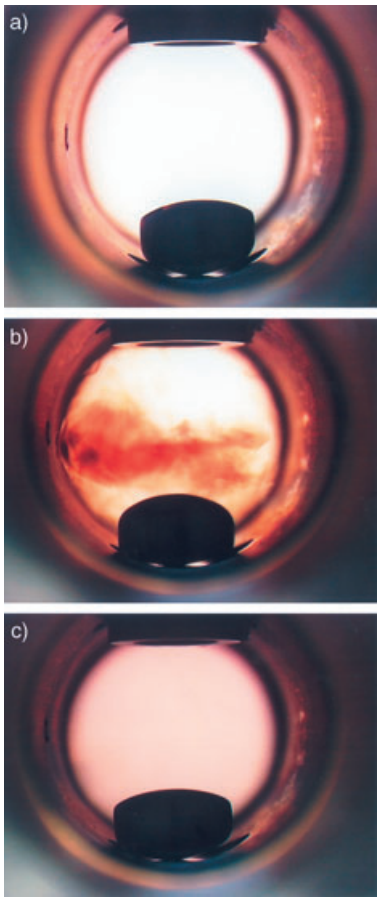

Figure 1. Digital photographs showing the formation of Ag nanoparticles in AOTF w/c RMs: a) RMs before the addition of the reducing agent, b) soon after the addition of the reducing agent, and c) the optically transparent Ag nanoparticle dispersions.

The UV/Vis absorption spectra showing the surface plasmon absorption of silver nanoparticles encapsulated in AOTF w/c reverse micelles are presented in Figure 2. It is seen that the broad surface plasmon absorption band ($\lambda_{max}=$ 415 nm) undergoes a slight red shift with increasing reaction time, which might be due to an increase in the size of the silver nanoparticles.[16] Additionally, the intensity of the silver nanoparticle absorption peak initially increased with time and reached its maximum in less than 3 min. Subse-

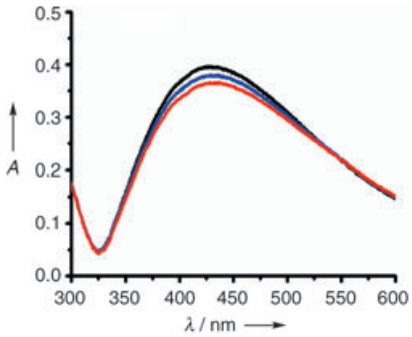

Figure 2. The surface-plasmon absorption spectra of silver nanoparticles, formed in AOT w/c RMs ($W=4.7$) at 38.0 °C and 34.50 MPa (the spectral background for the microemulsions has been subtracted). The spectra are taken 3 (black), 30 (blue), and 60 min (red) after addition of the reducing agent.

quently, there was a gradual decrease in intensity, perhaps indicating the slow flocculation of some silver nanoparticles in the system.

There is a linear variation of the full width at half-maximum (FWHM) of the absorption peak with the inverse of the silver nanoparticle diameter (D).[17] The size of silver nanoparticles encapsulated in AOT reverse micelles, in isooctane and in compressed propane, have been estimated previously from UV/Vis absorption spectra by using the correlation given in Equation (1) (where FWHM is in nanometers, and D is in angstroms).[3b,5c]

$$\mathrm{FWHM} = 50 + (2300/D) \quad (1)$$

If Equation (1) is employed here, and taking the in situ UV/Vis spectrum recorded at 3 min after injection of the reducing agent, the colloidal silver particle is estimated to be approximately 2.6 nm in diameter.

The silver nanoparticles synthesized were redispersed in ethanol (after decreasing the CO_2 pressure), resulting in a homogeneous, yellow–green solution. Alternatively, RESS (rapid expansion of supercritical solutions) could be used to overlay the nanoparticles onto substrates of interest.

The morphology and size distribution of the silver nanoparticles were investigated by using transmission electron microscopy (TEM). Figures 3a and b show TEM images of the silver nanoparticles. As we anticipated, based on the absorption data, characteristic spherical silver nanoparticles were observed with a relatively narrow particle size distribution (~3–11 nm range). The high-resolution TEM images of the particles indicate some interlinking between individual nanoparticles, possibly through the interdigitation of the surfactant tails (Figure 3b) of adjacent micelles. A histogram showing the particle size distribution corresponding to Figure 3a is presented in Figure 4. The mean particle diameter observed is 6.0 nm (standard deviation, SD = 1.3 nm), and more than 95% of the nanoparticles are in the size range from 4 to 8 nm. This shows that the aqueous cores of the w/c RMs can act as effective templates for the synthesis of relatively monodisperse metal quantum dots, and that the surfactant interfacial monolayer acts as a passivation contact for the stabilization of the silver nanoparticles formed inside these templates.

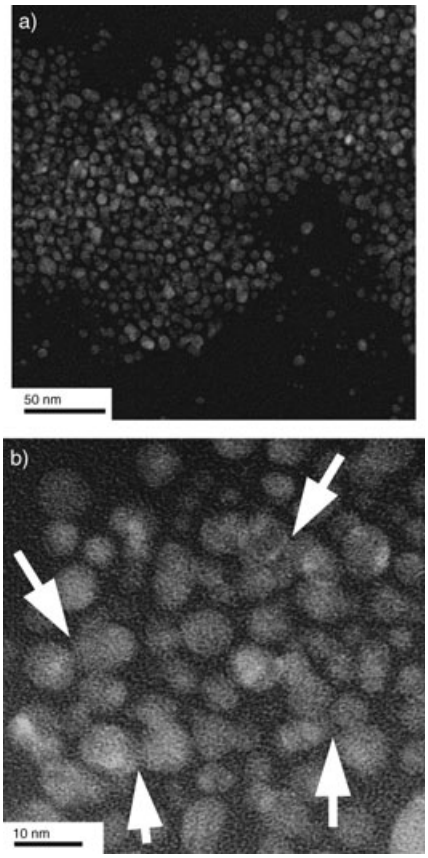

Figure 3. Representative TEM images of the Ag nanoparticles synthesized by AOT w/c RMs with $W=4.7$ at 38.0 °C and 34.50 MPa. Scale bars: a) 50 nm, b) 10 nm. The arrows point to the self-assembly of adjacent nanoparticles by means of the surfactant tails.

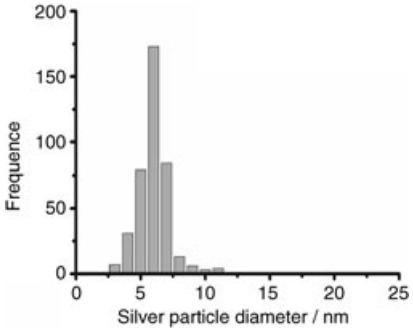

Figure 4. Histogram showing the size distribution of the silver nanoparticles corresponding to Figure 3a.

The multiple lattice fringes in the high-resolution TEM image (Figure 5a) suggest a high degree of crystallinity of the particles. To investigate the crystal structure of the silver nanoparticles prepared, the electron diffraction (ED) technique was used. Figure 5b shows the ED pattern of the silver nanoparticles; this pattern corresponds well to the crystal-

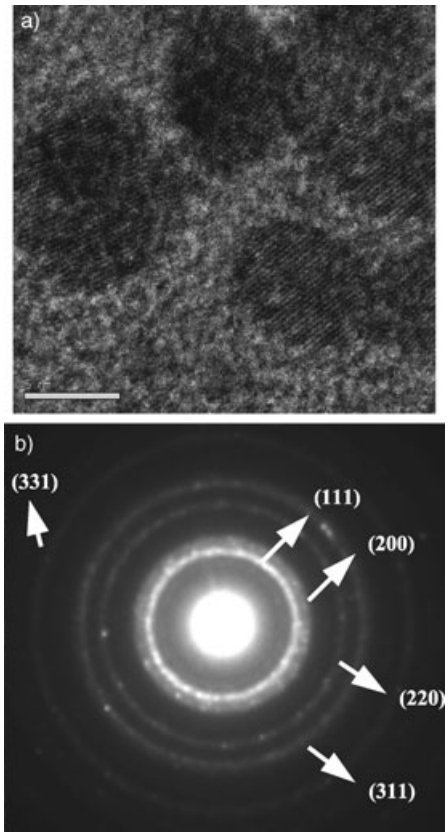

Figure 5. a) High-resolution TEM image (scale bar = 5 nm) and b) ED pattern of the Ag nanocrystals.

line planes of the face-centered-cubic (fcc) structure of the silver nanocrystals.

Silver iodide nanocrystals: Silver iodide (AgI) nanoparticles were synthesized by the reaction between silver nitrate and potassium iodide in the RM cores. Figure 6 shows the absorption spectra of AgI nanoparticles in the AOTF w/c RMs, along with the baseline corresponding to the RMs before injecting the KI aqueous solution. The characteristic absorption bands for AgI nanoparticles in the range of about 400–450 nm are observed. The maximum wavelength (λ_{max}) for the AgI nanoparticles increased with time after mixing, varying from 424 to 429 nm. About 3 min after mixing, λ_{max} reached almost a constant value of 429 nm. These spectra are consistent with the UV/Vis spectra reported previously.[14b,18] The absorption maxima in Figure 6 can provide a reasonable estimate for the size of the AgI nanoparticles. Since AgI is a direct-gap semiconductor, the absorption data was fitted to Equation (2) to determine the direct band gap energy.[19]

$$\sigma h\nu = \mathrm{A}(h\nu\text{-}E_g)^{0.5} \qquad (2)$$

σ is the molar absorption coefficient of AgI, $h\nu$ is the photon energy, A is a proportionality factor, and E_g is the band-gap energy. For a λ_{max} of 429 nm, the E_g value is estimated to be 3.12 eV. The diameter of the AgI nanoparticles can be estimated from the band-gap energy according to Brus's equation [Eq. (3)],[20] where $E_{g,bulk}$ is the bulk band gap, h is the Planck constant, d_p is the particle diameter, m_e is the effective mass of an electron, m_h is the effective mass of the hole, e is the charge of an electron, and ε_r is the dielectric constant of the semiconductor material. The particle diameter was estimated to be 3.4 nm by taking the E_g value calculated from Equation (2) and the following parameters for AgI: $E_{g,bulk} = 2.83$ eV, $\varepsilon_r = \varepsilon/\varepsilon_0 = 4.91$, $m^*/m_0 = 0.2$ (where ε is the permittivity of AgI, ε_0 is the permittivity of vacuum, m_0 is the rest mass of an electron, and $m^* = [1/m_e + 1/m_h]^{-1}$).

$$E_g = E_{g,bulk} + (h^2/2{d_p}^2)[1/m_e + 1/m_h] - [3.6e^2/4\pi\varepsilon_r d_p] \qquad (3)$$

A TEM image of the AgI particles is presented in Figure 7. In the case of AgI also, we observed the interlinking of the individual nanoparticles, possibly through the in-

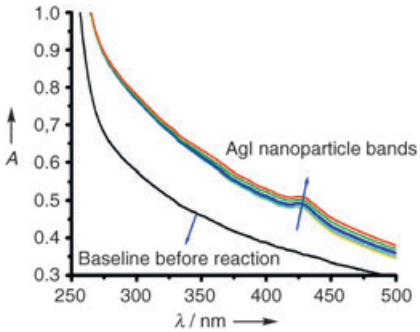

Figure 6. The surface-plasmon absorption spectra of the AgI nanoparticles prepared in AOTF w/c RMs with $W = 5.6$ at 38.0 °C and 34.50 MPa. The direction of the arrow on the AgI nanoparticle bands indicates absorption peaks at increasing time intervals (of 30 s) after injection of the aqueous KI solution.

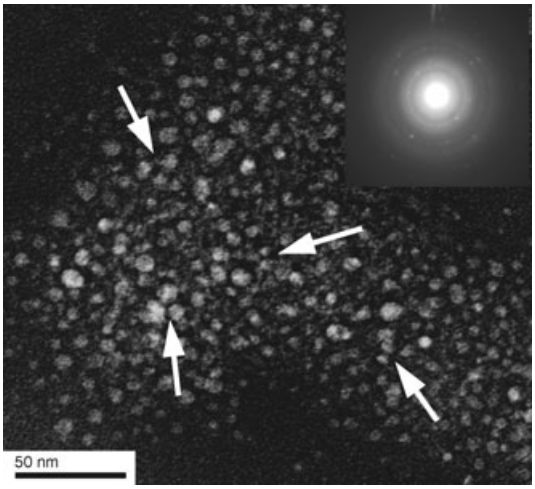

Figure 7. TEM image showing the AgI nanoparticles prepared in AOTF w/c RMs with $W = 5.6$ at 38.0 °C and 34.50 MPa. The arrows indicate the interaction between neighboring particles through the surfactant tails (scale bar = 50 nm). The inset presents the ED pattern for the corresponding particles.

terdigitation of the surfactant tails. The particle sizes were in the range of 3–10 nm, which was consistent with the particle size determined from the UV/Vis spectra. The ED pattern for the AgI nanoparticles prepared is also presented in Figure 7 (inset), and the diffraction rings suggest the formation of crystalline AgI particles. The particle size distribution histogram for the particles is presented in Figure 8, with

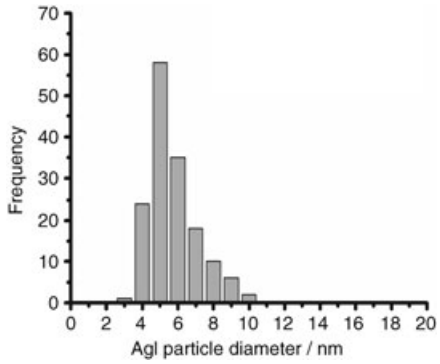

Figure 8. Histogram showing the size distribution of the AgI nanoparticles corresponding to Figure 7.

the mean particle diameter = 5.7 nm (SD = 1.4 nm). More than 94% of the silver iodide particles are in the narrow size range of 4 to 8 nm. Additionally, as can be seen from Figure 9, the multiple misaligned lattice fringes of the AgI nanoparticles, which seem to have surfactant molecules attached to them, could be observed clearly, further confirming the formation of AgI nanocrystals.

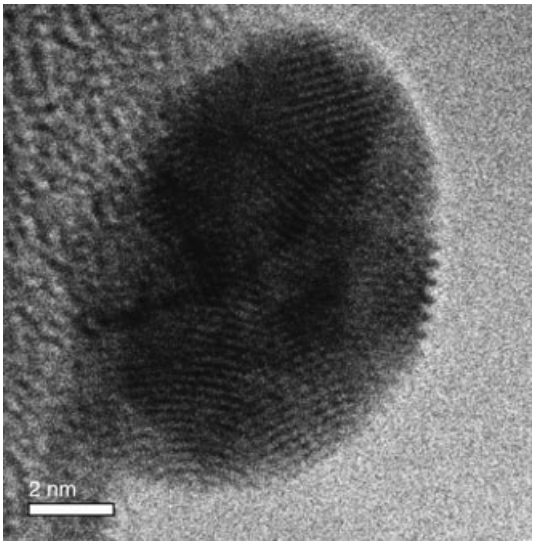

Figure 9. High-resolution TEM image of AgI nanocrystals (scale bar = 2 nm).

Mechanism: The exact nature of the diffusion mechanism of the reactants into the aqueous RM cores, and especially the role of F-pentanol in the RM system, is interesting and is a topic of our current investigation. The role of F-pentanol in the stabilization of the AOTF RM is to provide enhanced solvent interaction with the micellar tails. It is well known that fluorocarbons are highly CO_2-philic, because of the very low (much less than zero) dipolarity/polarizability parameters,[21] and are generally used as a molecular fragment to dissolve otherwise insoluble molecular functionalities in $scCO_2$. Simulations of molecular dynamics[22] clearly reveal significant solvent penetration into the fluorocarbon tail region of the micelles. We anticipated similar effects by utilizing a CO_2-philic fluorocarbon cosurfactant, which will interdigitate between the hydrocarbon tails and enhance the effective interaction cross section between the solvent and the tails, providing greater stabilization of the RM in $scCO_2$. The F-pentanol hydroxy groups interact with loading water molecules in the polar core regions by means of hydrogen bonds, and CO_2-philic fluorinated groups interact with CO_2 molecules, which penetrate from the bulk CO_2 phase into the surfactant tail region. Both of these interactions are beneficial for the F-pentanol molecule to insert itself between surfactant tails and reduce the electrostatic repulsion between the AOT ionic head groups, thereby enhancing the stability of the RM system.

The CO_2 pressures employed in the current experiment to stabilize the microemulsion systems are higher than those used for PFPE systems (25.0 MPa);[12b] this higher pressure may be attributed to a reduction in the effective solvation of the AOT tails in CO_2 in comparison with that of PFPE. However, the current system presents an economically viable and stable microemulsion system that can be utilized for the synthesis of metal and semiconductor nanoparticles. The particle size distributions obtained in the current experiments are also comparable (especially the relatively narrow size range) to that obtained by means of the PFPE system.

The dynamic assembly of the surfactant tails allows the diffusion of the reactants into the aqueous core and enables the reduction of the silver ions to their ground state within the polar nanometer-sized aqueous domains of the AOTF w/c RMs. Although the injection of aqueous or ethanolic solutions containing the reagents can, in principle, affect the size and stability of the micellar structure, we did not observe any phase separations upon injection into these systems, indicating that the microemulsion systems are stable under the experimental conditions. In addition, previous studies[14a] of the PFPE-PO_4-AOT mixed-surfactant systems indicated that the addition of ethanol, in fact, increases the stability of the microemulsion system and also the stability of the nanoparticles prepared. After nucleation is initiated, the particles grow, and the agglomeration of particles to a nanometer-sized particle takes place. The AOTF RMs in $scCO_2$ serve the function of an effective capping agent to passivate the particles' surfaces and quench particle growth, thereby leading to the metal and semiconductor nanoparticles, with an equivalent size to that of the micelle, being surrounded by a surfactant molecule monolayer.[23]

Conclusion

In this study, we have demonstrated the synthesis and stabilization of relatively monodisperse silver and silver iodide nanocrystals by chemical reactions within water-in-CO_2 reverse microemulsions; these nanocrystals were formed by using the commercially available AOT surfactant in the presence of a small quantity of inexpensive F-pentanol as cosolvent/cosurfactant at moderate temperature and CO_2 pressures. TEM results confirmed the formation of relatively monodisperse Ag and AgI nanocrystals with an average diameter of 6.0 nm (SD = 1.3 nm) and 5.7 nm (SD = 1.4 nm), respectively. Although the current experiments were restricted to the synthesis of metal and semiconductor nanoparticles, the approach can be expanded for a range of inorganic and organic reactions, especially for some important catalytic reactions (promoted by the in situ preparation of a highly effective nanosized metal catalyst), by using $scCO_2$ as a bulk phase.

Experimental Section

Materials: SCF-grade CO_2 (99.999% purity) was supplied by Nippon Sanso Company (Japan). AOT (99%, Sigma Ultra, MW = 444.56), purchased from Sigma Chemical Company (USA), was vacuum dried at 60°C for 24 h prior to use. F-pentanol and dehydrated ethanol were obtained from Tokyo Kasei Kogyo Company (Japan), and potassium iodide, silver nitrate, and double-distilled and de-ionized water (prepared by ultra-filtration, reverse osmosis, deionization, and distillation) were purchased from Wako Pure Chemicals Industries (Japan). $NaBH(OAc)_3$, which was used as a reducing agent in the study, was obtained from Aldrich Chemical Company.

Apparatus and procedures: Silver and silver iodide nanoparticles were characterized in situ by using UV/Vis absorption spectroscopy in a high-pressure cell, which was similar to the one reported previously.[24] The high-pressure UV cell consisted of a stainless-steel cell with two sapphire windows. It had a volume of 2.2 cm^3 and could withstand a maximum pressure of 45 MPa. The mixtures in the cell were stirred by a magnetic stirrer. CO_2 pressure was controlled by a back-pressure regulator (880–81, JASCO Co.) to an accuracy of 0.01 MPa in the pressure range of 0–50 MPa. All the measurements were carried out at 38.0(±0.1)°C.

Preparation of nanoparticles: Here, a typical experiment for the synthesis of Ag nanoparticles is described, the procedure for the synthesis of AgI nanoparticles being similar. The w/c RMs were prepared by adding AOT (0.016 M) and F-pentanol (0.24 M) to the UV cell, followed by an aliquot of silver nitrate aqueous solution (0.10 M) to achieve the desired amount of water. The cell was purged with gaseous CO_2 to remove the air and oxygen. $ScCO_2$ was pumped into the UV cell by a HPLC pump (PU-980, JASCO Co.) and thermal equilibrium was attained. The CO_2 pressure was raised with continuous stirring until single-phase, optically transparent w/c RMs were formed. The RMs containing silver ions were stirred continuously at 38.0°C and 27.00 MPa for one hour (the cloud-point pressure of the AOT (0.016 M)/F-pentanol (0.24 M)/water ($W = 4.7$)/$scCO_2$ mixture system is 26.77 MPa[15b]). The UV/Vis spectrum of the microemulsions was recorded and stored as a baseline. Then a freshly prepared solution of $NaBH(OAc)_3$ in ethanol was slowly injected, through a 20 μL sample loop, into the UV cell by using a high-pressure pump connected to a six-port valve (7125, COTATI, California, USA) until a final pressure of 34.50 MPa was achieved. Stirring was stopped after the addition of the reducing agent to allow spontaneous nucleation and growth of silver nanoparticles. The estimated concentrations of the silver nitrate and $NaBH(OAc)_3$ in the $scCO_2$ microemulsions were 30 mM and 15 mM, respectively, and the fluid phase contained 20 μL of ethanol. With respect to the synthesis of the silver iodide nanoparticles, a AOTF w/c RM (W = 2.8) was prepared at a CO_2 pressure of 31.00 MPa before injecting a KI aqueous solution, because the cloud-point pressure of the mixture system of AOT (0.016 M)/F-pentanol (0.24 M)/water (W = 5.6)/$scCO_2$ is 30.30 MPa.[15b] Thus, the introduction of the KI aqueous solution (W = 2.8) did not affect the stability of the AOTF w/c RMs, as the system pressure was high enough before the injection of the KI aqueous solution. The formation of the silver and silver iodide nanoparticles was monitored in situ by a Jasco V-570 UV/Vis spectrophotometer. A schematic diagram of the experimental setup for the synthesis and characterization of the colloidal silver and silver iodide nanocrystals by using UV spectroscopy is depicted in Figure 10. To observe the growth of the silver and silver iodide nanoparticles, a 10 mL high-pressure view cell[25] was used instead of the high-pressure UV cell.

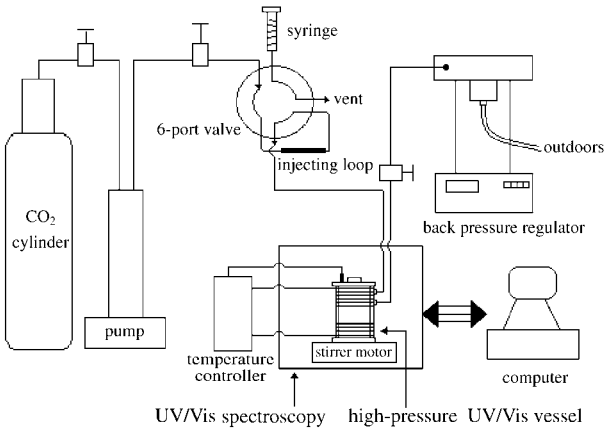

Figure 10. Schematic drawing of the experimental setup for the synthesis and spectroscopic characterization of nanoparticles in AOTF w/c RMs.

TEM and ED studies: The AOTF w/c RMs bearing the silver and silver iodide nanoparticles were depressurized slowly, and the nanoparticles in the cell were collected and re-dispersed in ethanol. Finally, the sample grids for TEM measurements were prepared by placing a drop of the ethanolic dispersion of nanoparticles onto the copper grid. The morphology and size distribution of the silver and silver iodide nanoparticles were determined by a Hitachi H-800 TEM at an operating voltage of 200 kV. The crystallinity of the silver and silver iodide nanoparticles was studied by electron diffraction techniques.

Acknowledgement

The authors are grateful to the Japanese Science Promotion Society (JSPS) for financial support.

[1] a) A. P. Alivisatos, *Science* **1996**, *271*, 933; b) C. N. R. Rao, G. U. Kulkarni, P. J. Thomas, P. P. Edwards, *Chem. Eur. J.* **2002**, *8*, 28; c) M. A. El-Sayed, *Acc. Chem. Res.* **2004**, *37*, 326.

[2] a) M. Brust, M. Walker, D. Bethell, D. J. Schiffrin, R. Whyman, *J. Chem. Soc. Chem. Commun.* **1994**, 801; b) A. Ullman, *Chem. Rev.* **1996**, *96*, 1533; c) A. C. Templeton, M. J. Hostetler, C. T. Kraft, R. W. Murray, *J. Am. Chem. Soc.* **1998**, *120*, 1906; d) P. S. Shah, J. D. Holmes, R. C. Doty, K. P. Johnston, B. A. Korgel, *J. Am. Chem. Soc.* **2000**, *122*, 4245; e) P. S. Shah, J. D. Holmes, K. P. Johnston, B. A. Korgel, *J. Phys. Chem. B* **2002**, *106*, 2545; f) P. S. Shah, S. Husain, K. P. Johnston, B. A. Korgel, *J. Phys. Chem. B* **2002**, *106*, 12178.

[3] a) M. L. Steigerwald, A. P. Alivisatos, J. M. Gibson, T. D. Harris, R. Kortan, A. J. Muller, A. M. Thayer, T. M. Duncan, L. E. Brus, *J.*

Am. Chem. Soc. **1988**, *110*, 3046; b) C. Petit, P. Lixon, M. P. Pileni, *J. Phys. Chem.* **1993**, *97*, 12974; c) J. P. Cason, M. E. Miller, J. B. Thompson, C. B. Roberts, *J. Phys. Chem. B.* **2001**, *105*, 2297; d) C. L. Kitchens, M. C. McLeod, C. B. Roberts, *J. Phys. Chem. B* **2003**, *107*, 11331; e) M. P. Pileni, L. Motte, C. Petit, *Chem. Mater.* **1992**, *4*, 338; f) M. Meyer, C. Wallberg, K. Kurchara, J. H. Fendler, *J. Chem. Soc. Chem. Commun.* **1984**, 90.

[4] a) K. S. Suslick, M. Fang, T. Hyeon, *J. Am. Chem. Soc.* **1996**, *118*, 11960; b) M. Zhao, L. Sun, R. M. Crooks, *J. Am. Chem. Soc.* **1998**, *120*, 4877; c) R. Wang, J. Yang, Z. Zheng, M. D. Carducci, J. Jiao, S. Seraphin, *Angew. Chem.* **2001**, *113*, 567; *Angew. Chem. Int. Ed.* **2001**, *40*, 549; d) P. Raveendran, J. Fu, S. L. Wallen, *J. Am. Chem. Soc.* **2003**, *125*, 13940.

[5] a) C. B. Roberts, J. B. Thompson, *J. Phys. Chem. B* **1998**, *102*, 9074; b) J. P. Cason, C. B. Roberts, *J. Phys. Chem. B* **2000**, *104*, 1217; c) J. P. Cason, K. Khambaswadkar, C. B. Roberts, *Ind. Eng. Chem. Res.* **2000**, *39*, 4749.

[6] a) M. A. McHugh, V. J. Krukonis, *Supercritical Fluid Extraction*. 2nd ed., Butterworth Heinemann, Boston, MA, **1994**; b) M. Poliakoff, P. King, *Nature* **2001**, *412*, 125.

[7] a) J. D. Holmes, K. P. Johnston, R. C. Doty, B. A. Korgel, *Science* **2000**, *287*, 1471; b) K. J. Ziegler, R. C. Doty, K. P. Johnston, B. A. Korgel, *J. Am. Chem. Soc.* **2001**, *123*, 7797.

[8] a) S. G. Kazarian, M. F. Vincent, F. V. Bright, C. L. Liotta, C. A. Eckert, *J. Am. Chem. Soc.* **1996**, *118*, 1729; b) J. F. Kauffman, *J. Phys. Chem. A* **2001**, *105*, 3433; c) P. Raveendran, S. L. Wallen, *J. Am. Chem. Soc.* **2002**, *124*, 12590; d) P. Raveendran, S. L. Wallen, *J. Phys. Chem. B* **2003**, *107*, 1473; e) A. Fujii, T. Ebata, N. Mikami, *J. Phys. Chem. A* **2002**, *106*, 10590.

[9] a) K. A. Consani, R. D. Smith, *J. Supercrit. Fluids* **1990**, *3*, 51; b) T. A. Hoefling, R. M. Enick, E. J. Beckman, *J. Phys. Chem.* **1991**, *95*, 7127; c) K. Harrison, K. P. Johnston, *Langmuir* **1994**, *10*, 3536.

[10] a) J. Eastoe, A. Paul, S. Nave, D. C. Steytler, B. H. Robinson, E. Rumsey, M. Thorpe, R. K. Heenan, *J. Am. Chem. Soc.* **2001**, *123*, 988; b) J. C. Liu, B. X. Han, J. L. Zhang, G. Z. Li, X. G. Zhang, J. Wang, B. Z. Dong, *Chem. Eur. J.* **2002**, *8*, 1356; c) J. C. Liu, B. X. Han, G. Z. Li, X. G. Zhang, J. He, Z. M. Liu, *Langmuir* **2001**, *17*, 8040; d) W Ryoo, S. E. Webber, K. P. Johnston, *Ind. Eng. Chem. Res.* **2003**, *42*, 6348.

[11] a) K. P. Johnston, K. L. Harrison, M. J. Clarke, S. M. Howdle, F. V. Bright, C. Carlier, T. W. Randolph, *Science* **1996**, *271*, 624; b) J. B. McClain, D. E. Betts, D. A. Canelas, E. T. Samulski, J. M. Desimone, J. D. Londono, H. D. Cochran, G. D. Wignall, D. Chillura-Martino, R. Triolo, *Science* **1996**, *274*, 2049; c) J. Eastoe, B. H. M. Cazelles, D. C. Steytler, J. D. Holmes, A. R. Pitt, T. J. Wear, R. K. Heenan, *Langmuir* **1997**, *13*, 6980; d) Z. T. Liu, C. Erkey, *Langmuir* **2001**, *17*, 274; e) J. S. Keiper, R. Simhan, J. M. DeSimone, G. D. L. Wignal, Y. B. Melnichenko, H. Frielinghaus, *J. Am. Chem. Soc.* **2002**, *124*, 1834; f) M. Sagisaka, S. Yoda, Y. Takebayashi, K. Otake, B. Kitiyanan, Y. Kondo, N. Yoshino, K. Takebayashi, H. Sakai, M. Abe, *Langmuir* **2003**, *19*, 220; g) J. Eastoe, A. Dupont, D. C. Steytler, *Curr. Opin. Colloid Interface Sci.* **2003**, *8*, 267.

[12] a) J. D. Holmes, P. A. Bhargava, B. A. Korgel, K. P. Johnston, *Langmuir* **1999**, *15*, 6613; b) M. C. McLeod, R. S. McHenry, E. J. Beckman, C. B. Roberts, *J. Phys. Chem. B* **2003**, *107*, 2693; c) K. T. Lim, H. S. Hwang, M. S. Lee, G. D. Lee, S. Hong, K. P. Johnston, *Chem. Commun.* **2002**, 1528.

[13] a) H. Ohde, M. Ohde, F. Bailey, H. Kim, C. M. Wai, *Nano Lett.* **2002**, *2*, 721; b) X. Dong, D. Potter, C. Erkey, *Ind. Eng. Chem. Res.* **2002**, *41*, 4489.

[14] a) M. Ji, X. Y. Chen, C. M. Wai, J. L. Fulton, *J. Am. Chem. Soc.* **1999**, *21*, 2631; b) H. Ohde, J. M. Rodriguez, X. R. Ye, C. M. Wai, *Chem. Commun.* **2000**, 2353; c) H. Ohde, F. Hunt, C. M. Wai, *Chem. Mater.* **2001**, *13*, 4130; d) H. Ohde, C. M. Wai, H. Kim, J. Kim, H. Ohde, *J. Am. Chem. Soc.* **2002**, *124*, 4540; e) M. Ohde, H. Ohde, C. M. Wai, *Chem. Commun.* **2002**, 2388.

[15] a) J. C. Liu, Y. Ikushima, Z. Shervani, *J. Supercrit. Fluids* **2004**, *32*, 97; b) J. C. Liu, Z. Shervani, P. Raveendran, Y. Ikushima, *J. Supercrit. Fluids* **2005**, *33*, 121.

[16] B. G. Ershov, A. Henglein, *J. Phys. Chem. B* **1998**, *102*, 10663.

[17] a) K. P. Charle, W. Schulze, *Ber. Bunsen-Ges. Phys. Chem.* **1984**, *88*, 350; b) M. P. Andrews, G. A. Ozin, *J. Phys. Chem.* **1986**, *90*, 2929.

[18] H. Sato, I. Komasawa, *J. Chem. Eng. Jpn.* **1996**, *29*, 501.

[19] Y. Wang, A. Suna, W. Mahler, *J. Chem. Phys.* **1987**, *87*, 73.

[20] L. E. Brus, *J. Chem. Phys.* **1984**, *80*, 4403.

[21] a) M. E. Sigman, S. M. Lindley, J. E. Leffler, *J. Am. Chem. Soc.* **1985**, *107*, 1471; b) C. R. Yonker, S. L. Frye, R. D. Smith, *J. Phys. Chem.* **1986**, *90*, 3022; c) T. A. Hoefling, D. Stofesky, M. Reid, E. J. Beckman, R. M. Enick, *J. Supercrit. Fluids* **1992**, *5*, 237.

[22] a) S. R. P. da Rocha, K. P. Johnston, P. J. Rossky, *J. Phys. Chem. B* **2002**, *106*, 13250; b) S. Senapati S. M. L. Berkowitz, *J. Phys. Chem. B* **2003**, *107*, 12906.

[23] J. C. Liu, P. Raveendran, Z. Shervani, Y. Ikushima, *Chem. Commun.* **2004**, 2582.

[24] Z. Shervani, Y. Ikushima, *Colloid Polym. Sci.* **1999**, *277*, 595.

[25] T. Kawakami, N. Saito, Y. Ikushima, C. C. Liew, K. Aiba, T. Ohkawa *Chem. Lett.* **2000**, *29*, 402.

Received: May 24, 2004
Revised: November 4, 2004
Published online: January 26, 2005